中国计量科学研究院
National Institute of Metrology,China

Activites on DC & LF Electricity and Magnetism at NIM

National Institute of Metrology, China
Contacts: *Dr. Qing He (heqing@nim.ac.cn)*

The New SI & Quantum Standards

- *The joule balance NIM-2*

Before the deadline of July 1st, 2017, the first determination of the Planck constant obtained with the NIM-2 in vacuum has been submitted to the Metrologia for publication. The measured Planck constant is 6.626 069 2(16) × 10^{-34} Js, which differs in relative terms by -1.27 × 10^{-7} from the CODATA 2014 value, with a relative standard uncertainty of 2.4×10^{-7}. However, this result is not used for the CODATA 2017 special adjustment because its uncertainty is bigger than 6×10^{-8}. The main uncertainty contributions are from the external field, alignment, and mass calibration, etc.

In 2018, to decrease the uncertainty contributions, a series of approaches have been performed to improve the NIM-2 joule balance to get an uncertainty of 10^{-8} level. We have redesigned and assembled several essential parts of the joule balance, including the mechanical lifting system of the exciting magnet, the shielding and compensating system of the external field, and the alignment measurement and adjustment system for the suspended coil. As to the mechanical lifting system, we have built new guide-rails and upper loading plates for a more stable motion mode during the up and down stages of the exciting magnet, just as shown in Fig.1.

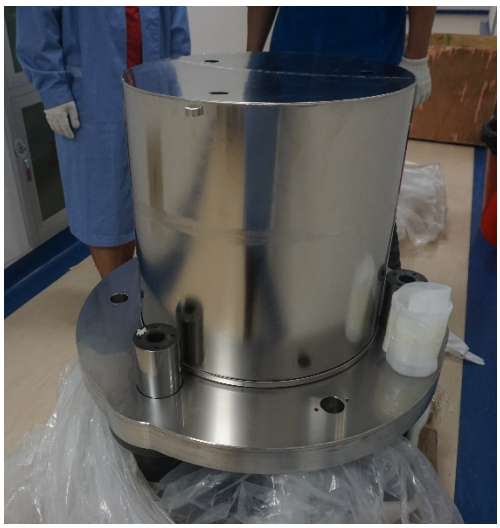

Figure 1. The new mechanical lifting system and the magnetic shield

Alignment is another important work for the joule balance to reach the 10^{-8} level measurement uncertainty. In the joule balance, the alignment for suspended structures includes three parts: alignment measurement, alignment modeling, and alignment adjustment, and all these parts have been significantly improved:

1) 6 degrees of freedom displacements based on our existing interferometer were measured, as shown in Fig. 2 a).
2) We have built an alignment model by decoupling the electro-magnetic force and torque to refresh the relationship among the initial position, pose and the parasitic displacements of the suspended coil. Just as shown in Fig.2 b)
3) We have designed and rebuilt the new suspended system in joule balance, as shown in Fig.2 c).

Because of the above improvements, the variations of the horizontal displacement x, y and the rotation angles θ_x, θ_y can be reduced from 6 μm, 6 μm, 4 μrad, 4 μrad to 1 μm, 1 μm, 1 μrad, 0.5 μrad, respectively, and no obvious changes in the rotation angles θ_z can be detected during the force on-and-off progress. Furtherly, we need to improve the alignment status stability during the whole measurement stage and the alignment status repeatability between the upward and downward forces.

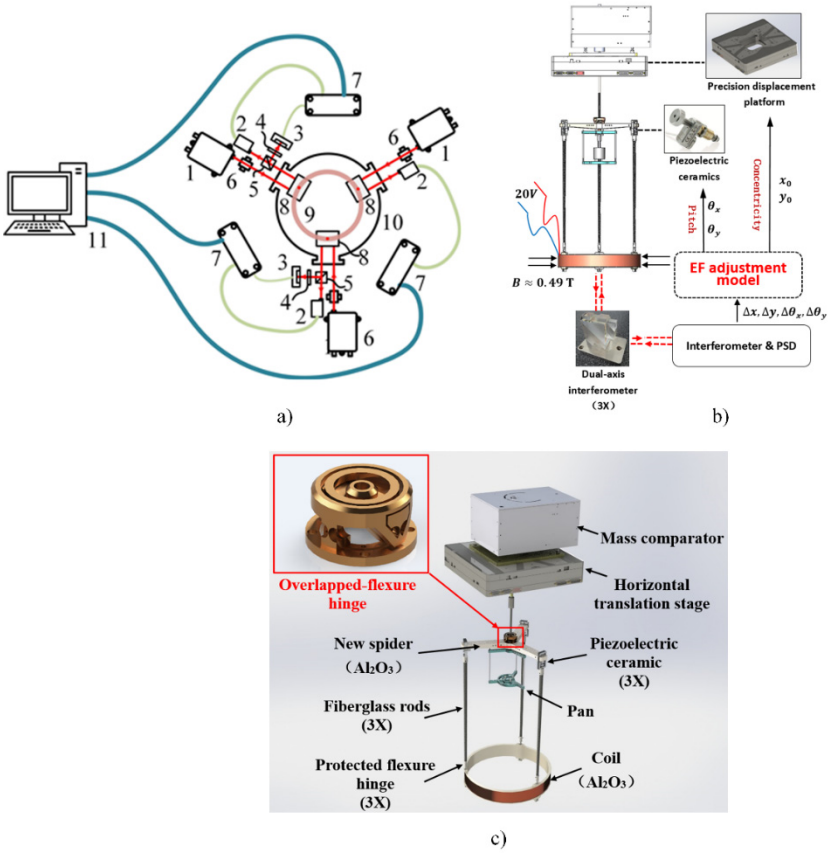

Figure 3. Schematic for alignment system of suspended coil in joule balance. a) Schematic for parasitic displacements measurement system of suspended coil in joule balance. 1. laser head, 2. receiver, 3. PSD, 4. polarizer, 5. BS, 6. steering optic, 7. signal process unit, 8. interferometer, 9. suspended coil, 10. vacuum chamber, 11. computer. b) Theoretical model for alignment. c) Schematic of the suspended structure in joule balance.

By the November 12th, the uncertainty of type A has been decreased to 10^{-8} level. Find adjustment and consistent improvement are still in progress.

Report Written by Dr. Zhengkun Li(lzk@nim.ac.cn), Division of Electromagnetism

- *Quantum Devices for electrical standards*

This year we mainly focus on two kind of devices: one is the Josephson junction (JJ) array devices for the quantum voltage standards, the other one is the nano-SQUID device which is for the inductive superconducting transition edge detector (ISTED). For the JJ devices, we have made the 0.5 V JJ array device which can produce 0.5 V quantum voltage. The device consists of about 14400 junctions and an on-chip Wilkinson microwave power divider. Our device is compared to the NIST device and good agreement is obtained. We also develop a new packaging scheme for the Josephson voltage chip. A chip with 400000 junctions (without transmission line) has been made and good dc I-V characteristics has been obtained. We are on our way to develop large scale DC/AC JJ arrays for the 1V or higher PJVS. Nano-SQUID is the read-out device for the ISTED. We have fabricated nano-SQUID devices by the e-beam lithography and reaction ion etch process as shown in the figure. The width of the nano-bridges was about 100 nm. The diameter of the loop was 20 μm. The working temperature range was from 7.0 K to 8.3 K. In the future, the absorbing layer such as Nb and NbSi films will be fabricated in the loop to form ISTED which will be used for the detection of single photon, X ray etc.

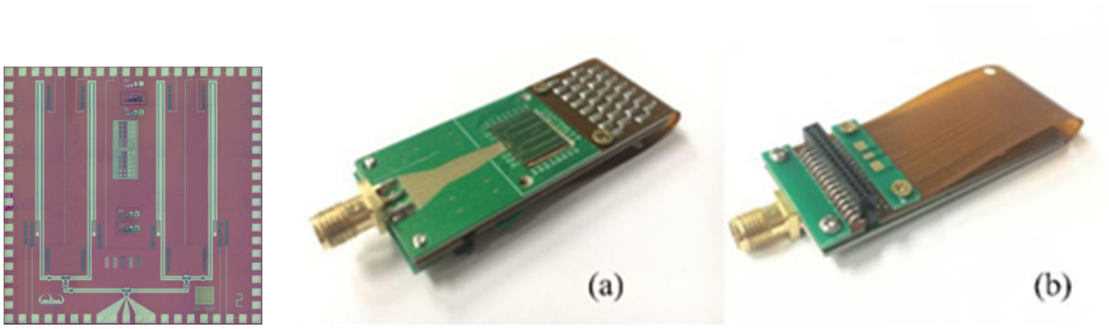

Figure 1. 0.5 V Josephson voltage standard chip

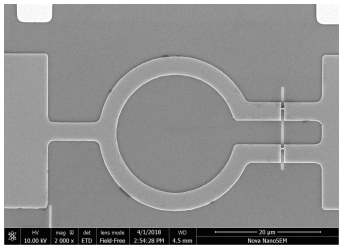

Figure 2. Nano SQUID

Report Written by Dr. Jinjin Li(jinjinli@nim.ac.cn), Division of Electromagnetism

- *Laser-pumped Cs-^{4}He magnetometer*

The Cs-^{4}He magnetometer (CHM) have been suggested to use to construct for magnetic flux density standard because of its advantages of no light shift error, linear response and insensitive to the fluctuations from the temperature, light and modulation intensity. In 2018, we build a CHM with using a single-mode laser to replace the traditional discharged lamp and improve the performance. The experimental setup is shown in Fig.1. The home-made Cs-^{4}He mixture cell is cylindrical with 4 cm diameter and 4 cm length, and is filled with a drop of Cs and 2.6 Torr ^{4}He. The Cs atoms are pumped by a signal mode DBR diode laser. The metastable ^{4}He atoms are produced by a 50 MHz pulse discharge microwave. An oscillating field B_{rf} with the direction perpendicular to that of the beam is added to produce the magnetic-resonance signal (MRS). The MRS can be detected by monitoring the absorption of the pump beam.

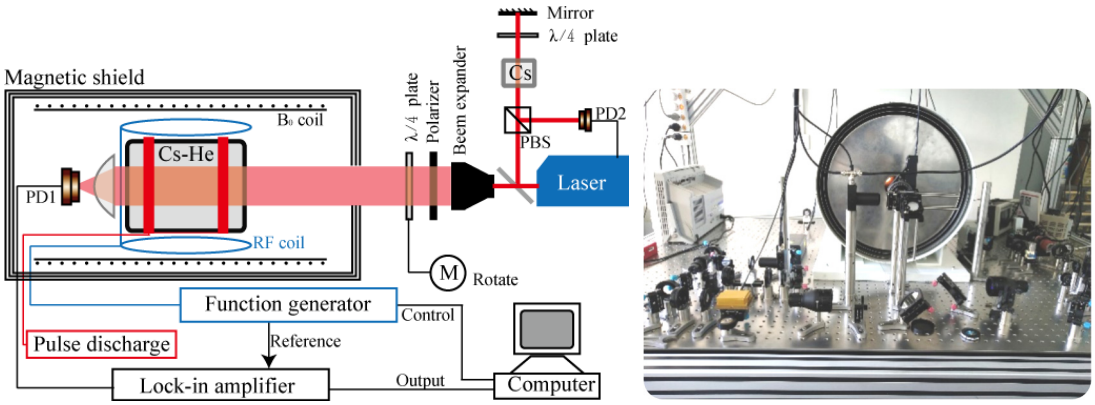

Fig. 1. Block diagram (left) and apparatus (right) of the laser-pumped CHM.

With the optimum light intensity and the optimum parameters of the pulsed discharge, the conversion slope of the laser-pumped CHM is 12.3 A/T, which has improved the conversion slope with an order of magnitude compare with the lamp-pumped CHM. By adding the plasma heating, the light shift can be deduced to the noise floor with sacrificing the SNR, which is about 0.03 nT. Further detail studies about the metrological features of this CHM will be study.

Report Written by Dr. Jiqing Fu (fujq@nim.ac.cn), Division of Electromagnetism

Impedance

- *The NIM's new Calculable Capacitor and the key comparison of capacitance (CCEM.K4.2017)*

The new NIM's calculable capacitor has been improved quit a lot since 2014. With the applying of NIM's unique electrical compensation method, the Calculable Capacitor's standard uncertainty of 10.5 × 10^{-9} has been achieved in 2018.

The key comparison of 10 pF and optional 100 pF capacitance has been carried out in 2017. A 'star' method is adopted where all participants sent their own AH capacitance standards to the pilot BIPM. The comparison has been completed within a short period of time and the results are excellent. The CCEM-K4 report has been just approved in Nov. 2018. NIM achieved a very good consistency of the comparison results.

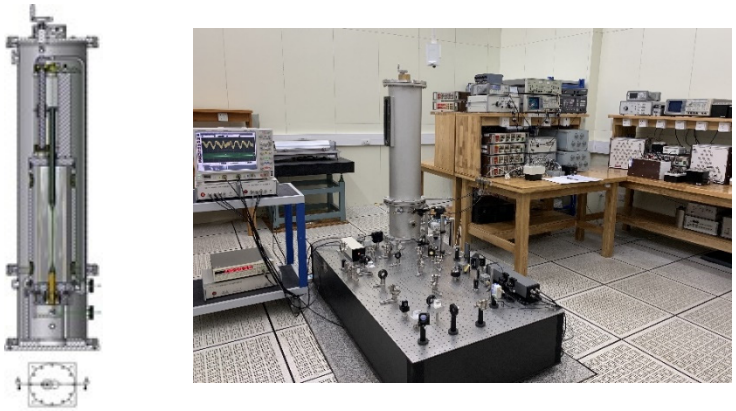

Figure 1. NIM's new Calculable Capacitor

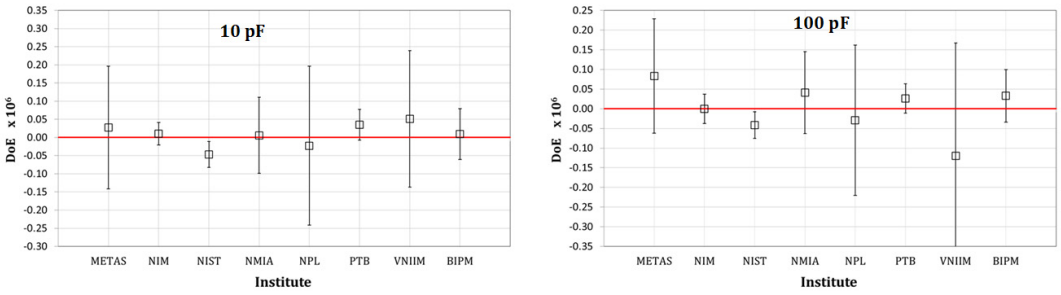

Figure 2. The CCEM-k4 comparison results of 10 pF and 100 pF

Report Written by Dr. Yan Yang(yangyan@nim.ac.cn), Division of Electromagnetism

- *New Haddad Calculable Resistor standard*

In 2018 we developed two new Haddad calculable resistor in cooperation with the BIPM. There are two different value of 1 kΩ and 1.2906 kΩ and their calculation for the a.c./d.c. differences are all less than 1×10^{-9} below 4 kHz. With the new four terminal-pair resistance bridge developed by BIPM, the measured difference for the frequency dependence is less than 5 $\times10^{-9}$ up to 3 kHz between the new Haddad calculable resistor of NIM and the previous Haddad calculable resistor of BIPM.

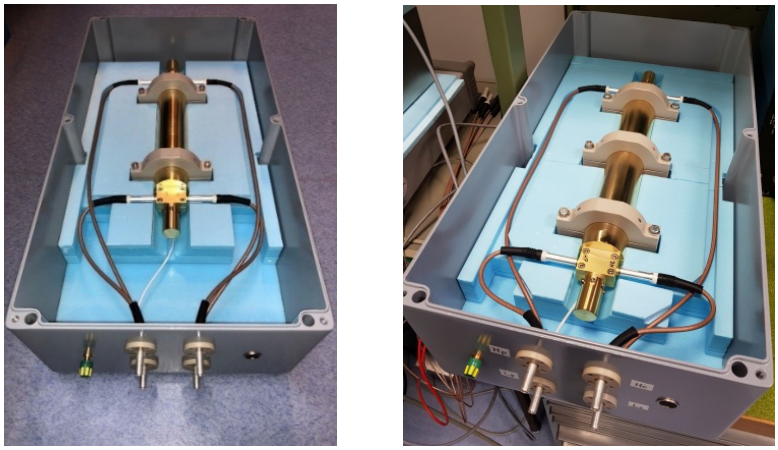

(a) (b)

Fig1. The two new Haddad calculable resistors with the nominal value of (a) 1 kΩ and (b) 1.2906kΩ

Report Written by Dr. Lu Huang(huanglu@nim.ac.cn), Division of Electromagnetism

AC Power and Energy

- *Activities on the calibration of EV charging Facilities*

In 2018, two national verification regulations of *AC Charging Spot for Electric Vehicles* and *Off-board Charger for Electric Vehicles* which were led by NIM have been issued by AQSIQ and have been mandatory since May 27, 2018. In the two regulations, operating errors are defined, considering that charging spots and off-board chargers should be verified on-site, and the range of ambient temperature is wider. Verification items and verification methods are given in the two regulations.

Figure 1. Fielding Calibratiing of EV Charging Spot with virtual load facilities

Figure 2. The Electric vehicle (EV) charging

Because large-scaled simultaneous charging of EVs brings great impact on grids, it causes the dynamical current and power. The precise measurement of electric energy under dynamical power is carried out. NIM propose the amplitude-modulation waveform as the abstraction of on-site variation, and use the waveform as testing waveform. We propose the inter-harmonics analysis method for measuring the power of amplitude-modulation waveform.

$$i(t) = (a + b\sin(2\pi ft / M))I_m \sin(2\pi ft)$$

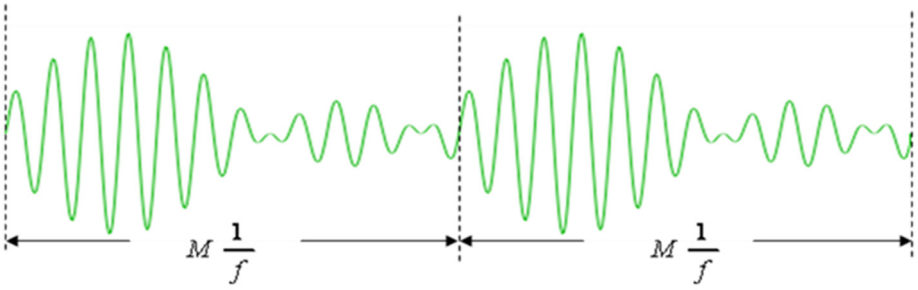

Report Written by Dr. Hongtao Huang(hht@nim.ac.cn), Division of Electromagnetism

- *AC Power standard Based on AC PJVS*

In 2018, NIM developed a power measurement system based on a PJVS. The measurement of two AC voltages were realized by means of a time-division measurement. Through automatically adjusting the phase, the sinusoidal signal intersects with the center position of the step. By analyzing the error sources of the differential sampling system, we provide theoretical help for circuit component parameter selection. If the RMS amplitude error is less than 0.1 μV/V, the system gain error in the circuit design will be less than 92 μV/V. When analyzing the zero-phase differential sampling, the fluctuation is less than 0.1 μrad in 4 days. We revise the amplitude and phase error of the RVD and I-V converter. The comparison with LIA shows that the differential sampling system has very good amplitude and phase measurement accuracy. The amplitude measurement difference between the DSS and LIA is less than 0.1 μV, and the phase measurement difference between the DSS and LIA is less than 0.1 μrad. The error difference between this and the national AC power standard is less than 2 μW/VA in 1.0, 0.5 L, and 0.5 C, and the values of En are less than 1. The results prove that the system performs well in power measurement.

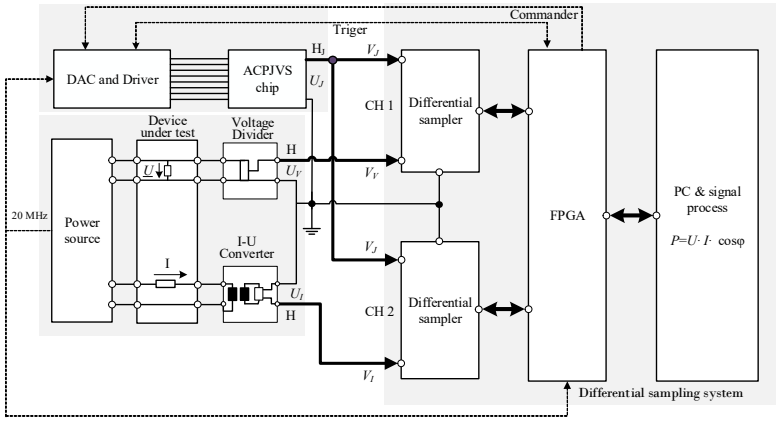

Fig. 1. AC power measurement system block diagram

Fig. 2. PJVS drive system

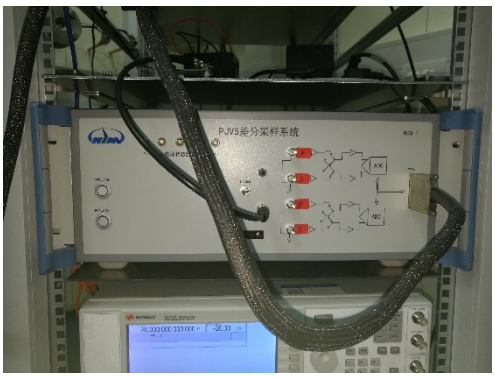

Fig. 3. Differential sampling system

Report written by Dr. Zhengsen JIA (jiazs@nim.ac.cn), Division Electromagnetic.

- *High frequency power*

A set of cascaded inductive voltage dividers (IVDs) with ratio of 2n:1 and resistive voltage dividers (RVDs) with serial-parallel connection structure have been developed in this year. The IVD with ratio of 2n:1 is built with a 2n-1:1 IVD and a binary IVD (BIVD) connecting in cascade structure. The phase angle errors of the IVDs are calibrated in a step-up procedure by using the three BIVDs in cascade connection as the reference standard. The phase angle errors of the RVDs can also be self-calibrated. The self-calibration results and uncertainties in phase angle errors of the IVDs and RVDs have been both given at frequencies up to 100 kHz. A closure measurement between the IVD with ratio of 256:1 and the RVD with ratio of 257:1 has also been done at frequencies from 25 kHz to 100 kHz. The closure results show good agreement within 15 μrad by comparing with the self-calibration results.

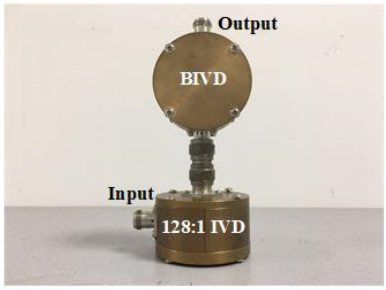

Fig 1. Cascade IVD with ratio of 256 to 1

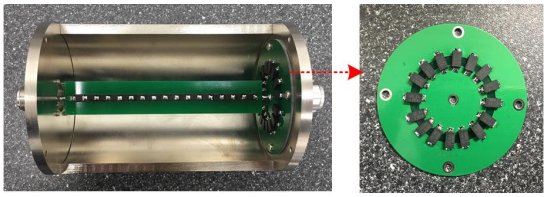

Fig 2. Serial-Parallel RVD with ratio of 257 to 1

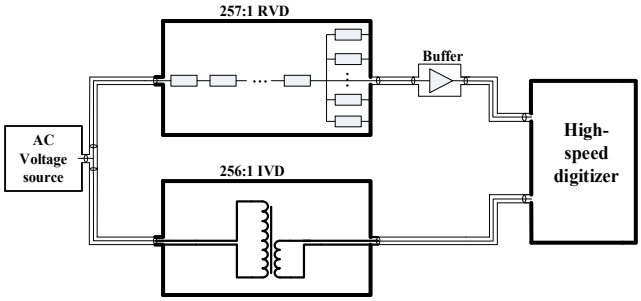

Fig 3. Comparison setup

Table I

CALIBRATION RESULTS AND MEASUREMENT RESULTS IN PHASE ANGLE DIFFERENCE BETWEEN TWO VDS

θ (μrad)	25 kHz	50 kHz	75 kHz	100 kHz
$\Delta\theta_C$	-1335	-2650	-3972	-5293
$\Delta\theta_M$	-1332	-2655	-3980	-5304
Δ	-3	5	8	11

The calibration and measurement results in phase difference between the two VDs are shown in Table I. The phase difference from self-calibration results, marked as ΔθC, agreed well with the measurement results ΔθM and the inconsistency is less than 15 μrad at frequencies up to 100 kHz.

Report Written by Dr. Jiangtao Zhang (zhangjt@nim.ac.cn)

High Voltage and Current

- *High voltage ratio for power frequency*

The voltage coefficient of a 400 kV compressed gas standard capacitor has been measured by simple tilting method. On this basis, a new method has been put forward to measure the coefficient of high voltage coefficient with CCD photography. The whole setup has been developed, and will be test in real capacitors by the end of this November. This method has been supposed to reduce the heavy work in the measuring of the tilting method significantly.

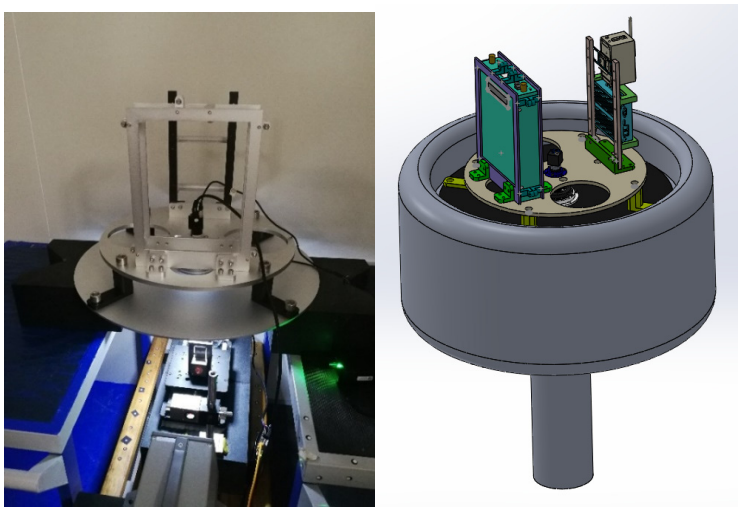

Fig1. High voltage capacitor

Report Written by Dr. Jiafu Wang (jiafu.wang@nim.ac.cn)

- *Measurement of transformer loss*

Two new projects on very low power factor measurement for power transformer and high voltage energy under nonlinearity loads in distribution grid start, which aims to resolve the loss and energy accurate measurement under low power factor, 10kV to 35kV or nonlinearity loads.

Basic model of Transformer Loss Measuring System had been built in NIM, with a research project supported by Chinese Ministry of Science and Technology approved in 2017. Currently, the research works focus on improving the stability and accuracy of these components, to utilize a standard system with the uncertainty of 40 ppm (k=2) for loss measurement at the power factor as low as 0.001.

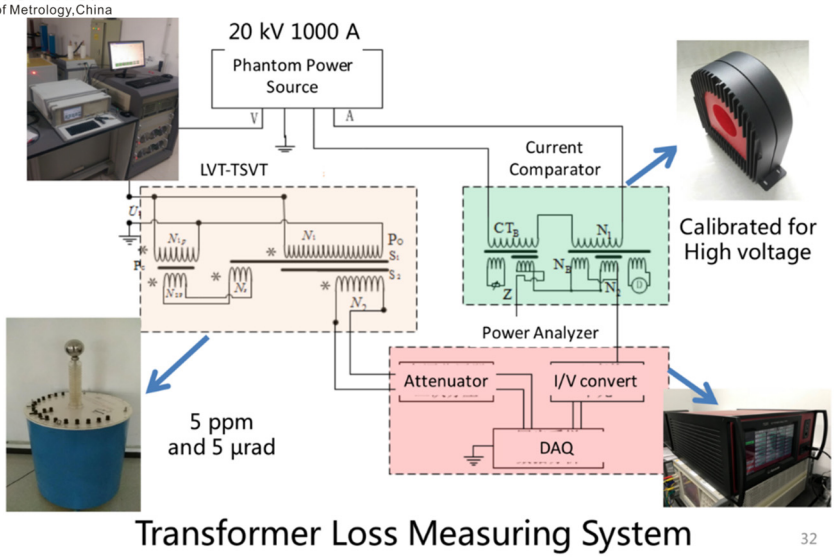

Report Written by Dr. Wei Zhao (zhaowei@nim.ac.cn)

- *Wideband fiber-optic current sensor*

A portable fiber-optic current sensor (FOCS) based on Faraday magneto-optical effect was developed, which intended to establish the DC, power frequency and long-pulse ultra-high current traceability for online and onsite calibration for metal electrolytic industry and power equipment testing.

The nonlinearity mechanism for the high current measurement of the FOCS using the closed-loop signal-detecting technology was deeply investigated. The 150kA DC high current calibration system was established. Based on the range self-expanding characteristic, the sensor calibration was achieved up to 300kA.

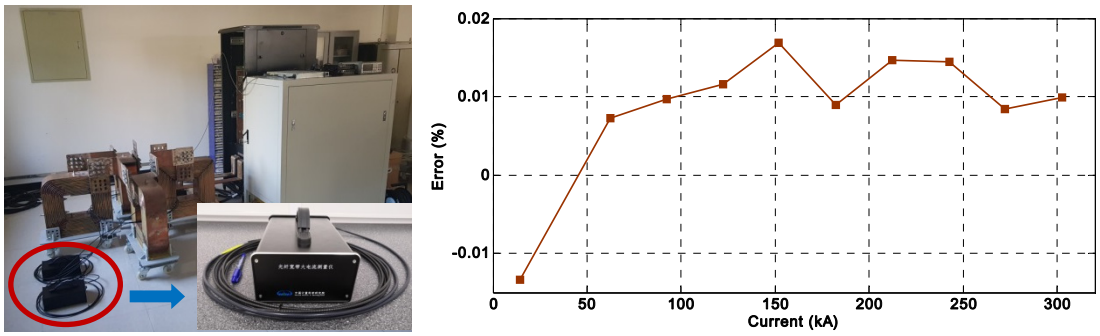

Fig 1. The portable fiber-optic current sensor and testing results

Report Written by Dr. Chuansheng Li (lichsh@nim.ac.cn)

中国计量科学研究院
National Institute of Metrology,China

Activities on RF metrology at NIM

National Institute of Metrology, China
Contacts: *Mr. Qiulai Gao(gaoql@nim.ac.cn)*

- ***RF Metrology***

- *RF Power Metrology*

NIM completed the design and fabrication of a WR‐5 (140 to 220GHz) thermos-electrical power sensor, power meter and microcalorimeter in 2018. That hardwarewill work together as the power primary standard and provide traceable power measurement in the range of 140 to 220GHz in China.

The self-designed power sensor has very low return loss (<-20dB), low signal leakage (-65dB) that can work as a transfer standard. The effective efficiency of the transfer standard over the full frequency band can be measured in the microcalorimeter. And the measurement uncertainty has been under evaluation.

In 2018, a Type N power standard system including power meter, a microcalorimeter and self-designed system control soft has been delivered to National Metrology Centre of Singapore (NMC) and Hong Kong Standards and Calibration Laboratory (SCL).

Type N Power Standard System

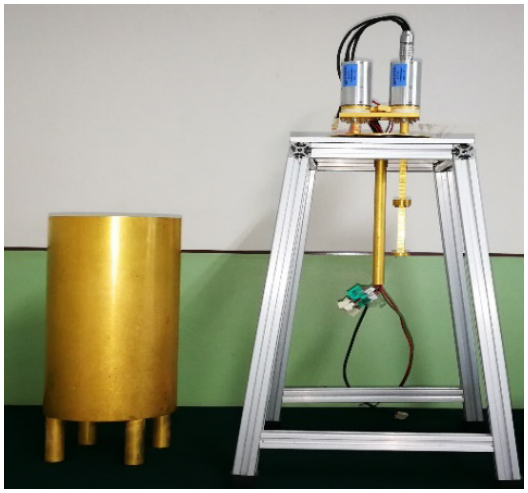

WR-5(140GHz~220GHz) Power Standard

Report Written by Dr. Xiaohai Cui (cuixh@nim.ac.cn)

- *Materials Metrology*

Based on the transmission/reflection method, the measurement system for characterizing the complex permittivity of materials in the frequency range from 100MHz to 40GHz was established by using the waveguide and coaxial line fixture. The relative standard uncertainty of the real part of the permittivity was lower than 1.0% with values of ε' lower than 20. An air-gap self-correction method was proposed to quantitatively eliminate the influence of air gap on transmission line method based on electromagnetic finite element simulation and optimization algorithm. In addition, in order to solve the problem of accurate measurement of low-loss materials, a novel method by using the two-channel transmission coefficient measurement system was proposed. Compared with the VNA-based measurement results, the measurement uncertainty of the loss tangent was reduced by an order of magnitude.

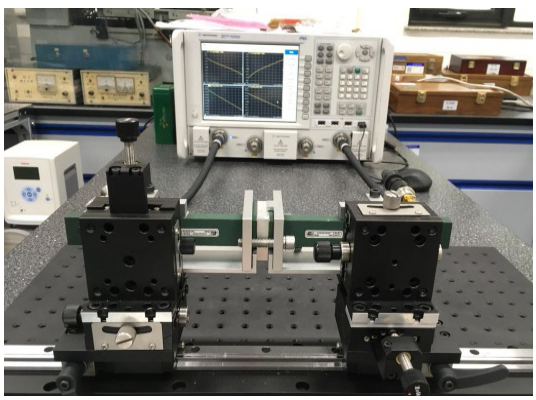

The transmission line measurement system based on the waveguide fixture

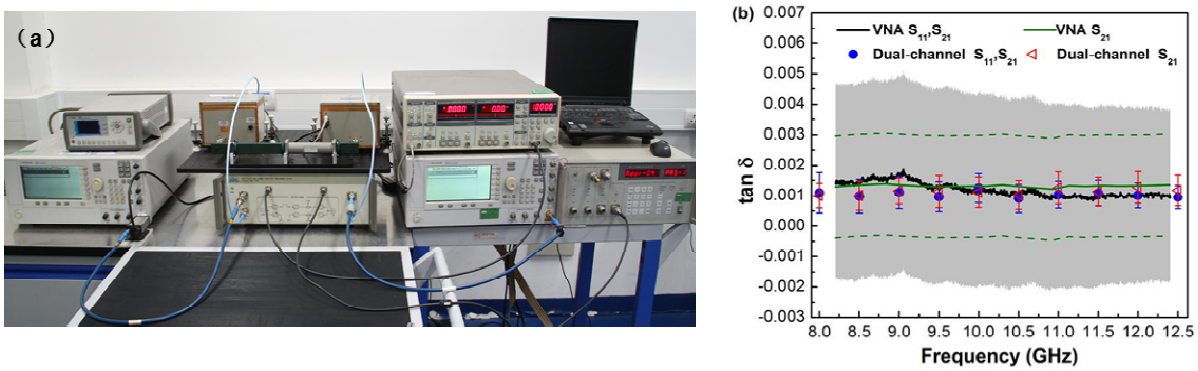

a) The dual-channel system for the measurement of low-loss material; b) The comparison of measurement results of loss tangent for polyimide aerogel between the dual-channel system method and VNA method.

Report Written by Dr. Hao Xu (xuhao@nim.ac.cn)

- *Scanning near-field microwave microscopy*

The scanning near-field microwave microscopy was developed in 2018, which was used to perform quantitative measurements of the local permittivity and conductivity of materials at nanoscale. The microwave probe was designed based on a quartz tuning fork glued with the electrochemically etched metal wires. The system is operated under the frequency modulation mode, which ensures satisfactory feedback stability on the tip-sample distance. The sensitivity and signal-to-noise-ratio of the measurement were improved by a two-port interferometric matching circuit. Detailed calibration method and uncertainty analysis are in progress.

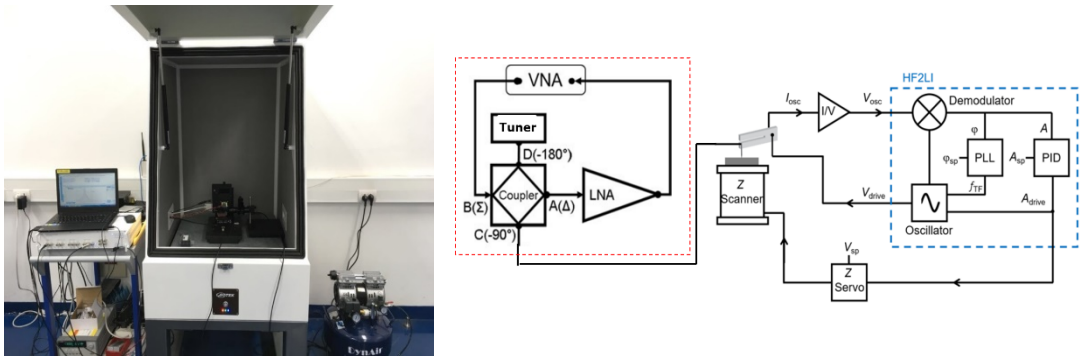

a) Experimental setup; b) Illustration of the scanning near-field microwave microscopy.

Report Written by Dr. Hao Xu (xuhao@nim.ac.cn)

- *Pulse Waveform Metrology*

An ultrafast pulse waveform system basing on electro-optic sampling technique was completed in 2015. The precise measurement of the 100GHz pulse waveforms were achieved using the LiTaO3-based electro-optic modulators with coplanar waveguide structure. The obtained rise time of impulses and step responses are 2.5 ps and 3.4 ps, respectively. The uncertainty analysis is in progress and a novel pulse waveform standard in NIM is being prepared.

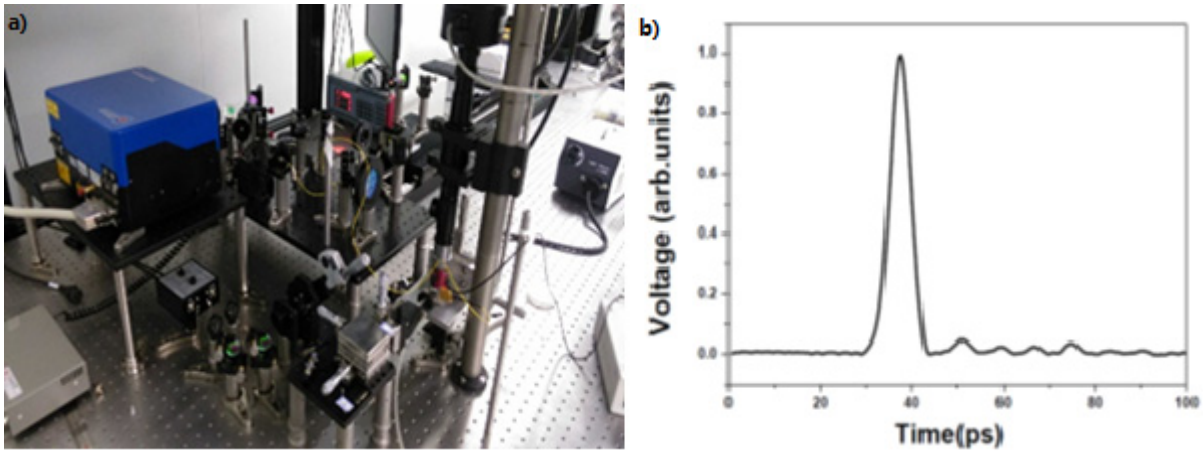

a) Experimental Setup; b) the 100 GHz time-domain pulse waveform basing on electro-optic sampling technique.

Report Written by Dr. Zhigang Feng (fengzgt@nim.ac.cn)

- *Quantum-based SI-traceable RFE-field Metrology*

The atom-based quantum physics will bring revolutionary improvement in radio frequency (RF) precision measurement and metrology, as in other metrology fields. The quantum coherence effects induced by RF field in highly-excited Rydberg atoms provide a revolutionary solution for RF E-field measurement. By using that, the RF E-field can be directly traced to optical frequency measurement and the Plank's constant.

The project of developing SI-traceable quantum RF metrology standards in the coming new SI definition was launched at the National Institute of Metrology (NIM) in 2015. At present, the practical measurement covers from 8.6 GHz to 93.7 GHz, with a sensitivity of 20 mV/m, and the deviation with respect to the calibrated field can be controlled within (0.5~2) %. The systematic investigation of uncertainty evaluation starts is still on the way.

In addition, the feasibility of some interesting applications has been verified at NIM, including the sub-wavelength field imaging and wireless communication. Developing RF metrology standards by using atom-based quantum effects is a valuable attempt in the new SI definition.

a) Experimental Setup; b) The room-temperature atomic vapor cell is used as a quantum probe for detecting RF E-field.

Report Written by Dr. Zhenfei Song (Songzf@nim.ac.cn)

The novel antenna：“optical feeding antenna”

A novel optical feeding antenna was developed in NIM in 2018. Usually, a RF coaxial cable is connected to a microwave antenna. However, due to the high loss, and high cost of coaxial cables, it is not convenient for massive antenna array or distributed antennas. Additional, for small antennas such as UWB PCB antennas, the coaxial cable will drastically disturb the radiation pattern, due to the common mode disturbance. We developed an optical feeding antenna and antenna array. The radiation pattern of the antenna array can be set through adjustment of the time delay of the optical cable.

The novel optical feeding antenna can operate from 500 MHz to 6 GHz, with a LNA is embedded into it. It can operate from 500 MHz up to 12 GHz when a broader band LNA is used.

中国计量科学研究院
National Institute of Metrology,China

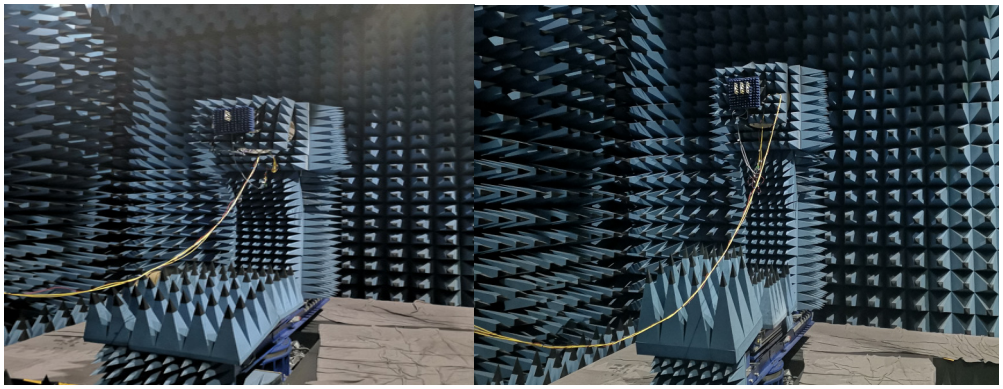

(a) a single “optical-feeding antenna” (b) three optical-feeding-antenna array

The measurement of optical feeding antennas

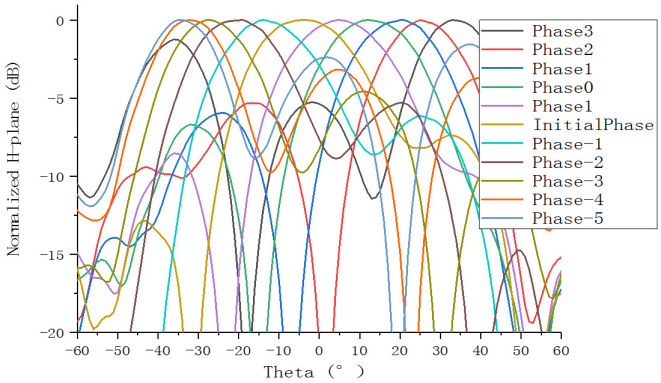

The radiation pattern of a phase controlled optical feeding antenna array

Report Written by Dr. Donglin Meng (mengdl@nim.ac.cn)